Engineering Structures 213 (2020) 110576

Contents lists available at ScienceDirect

Engineering Structures

journal homepage: www.elsevier.com/locate/engstruct

Experimental investigations on the load-carrying capacity of digitally produced wood-wood connections

Julien Gamerro[a,*], Jean Francois Bocquet[b], Yves Weinand[a]

[a] Ecole Polytechnique Fédérale de Lausanne (EPFL), School of Architecture, Civil and Environmental Engineering (ENAC), Institute of Civil Engineering (IIC), Laboratory for Timber Constructions (IBOIS), GC H2 711, Station 18, 1015 Lausanne, Switzerland

[b] École Nationale Supérieure des Technologies et Industries du Bois (ENSTIB), Laboratory for studies and research on wood material (LERMAB), 27 rue Philippe Séguin CS60036, 88026 Epinal cedex, France

ARTICLE INFO

Keywords:
Digital fabrication
Timber structures
Timber joints
Wood-wood connections
Load-carrying capacity
Shear test
Compression test
Design guidelines

ABSTRACT

The rise of digital fabrication has increased the use of wood-wood connections inspired by traditional carpentry in modern timber constructions. With recent developments on standard construction systems, the mechanical behavior of such joints for in-plane loading configurations is an essential parameter for the structural design. However, only few design guidelines exist on this topic in building codes such as Eurocode 5 and research has been mainly focused on the rotational behavior, which is important for free-form structures. Therefore, this work presents an experimental campaign on the load-carrying capacity of digitally produced through tenon connections for commonly available engineered timber products such as oriented strand board, laminated veneer lumber, and multiply solid wood panels. Shear and compression failure modes were studied and two test setups were developed. The scope of the study was limited to five different materials, a grain orientation parallel to the joint, and three different tenon lengths. The test results showed significant differences between the product specifications given by manufacturers and real performances observed for oriented strand board and cross laminated timber, while laminated veneer lumber had more accurate specifications. Nonetheless, a spreading of the compression strength was highlighted only for the OSB material and was also observed for the shear strength of laminated veneer lumber specimens. The existing Eurocode 5 guidelines generally underestimated the load-carrying capacity of the connections by 25% and only the capacity of oriented strand board connections was overestimated. Finally, the study demonstrates that different design approaches can be defined according to the material employed in through tenon connections. Design diagrams based on tests are preferred for materials with a high variability between product specifications and real performances while design criteria from building codes can be applied for the others.

1. Introduction

The emergence of digital fabrication has led to new developments for the use of traditional wood-wood assemblies in timber constructions [1]. The workflow from design to production has considerably evolved in the last decades [2] and a large number of connections with various geometries can now be easily manufactured. Automation and new production tools such as computer numerical control (CNC) machines have made traditional wood-wood assemblies a cost competitive alternative to bonding and steel fasteners for modern structures. Several research works have thus been performed on this topic using different types of connections and have led to prototypes as well as pavilions for complex geometries [3–5]. The feasibility of this construction technique has been proven with the first large-scale structure using through tenon (TT) connections [6] while another is planned to be achieved in 2020 [7]. TT connections are based on traditional tenon-mortise assemblies, which are composed of a male part (tenon) inserted in a female part (mortise). The mechanical behavior of TT connections has been mainly studied in rotation because of the particular origami or free-form shapes of these structures [8,9]. However, with the increasing interest in timber elements interconnected by wood-wood connections, TT joints are now used for the development of basic housing systems such as orthogonal roof or slab components [10,11], where the load-carrying capacity for in-plane loads is an essential parameter for the structural design. Therefore, this paper focuses on the mechanical characterization of TT connections for this type of loading configuration.

A new construction system for interconnected timber elements

* Corresponding author.
E-mail address: julien.gamerro@epfl.ch (J. Gamerro).

https://doi.org/10.1016/j.engstruct.2020.110576
Received 6 February 2020; Received in revised form 20 March 2020; Accepted 24 March 2020

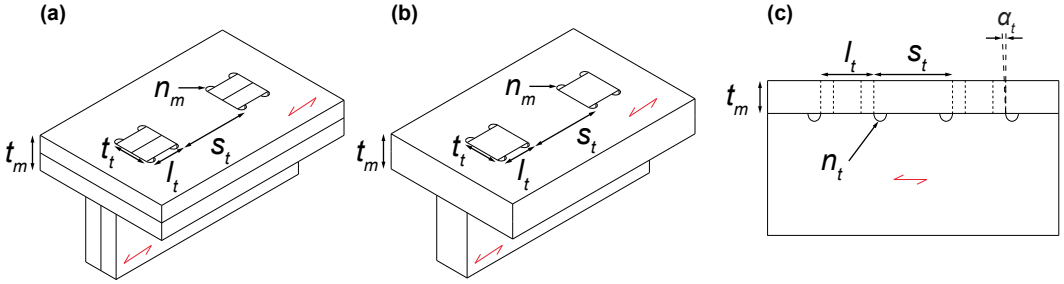

Fig. 1. Geometry and parameters of a TT connection: (a) Axonometry of a double-layered connection/ (b) Axonometry of a single-layered connection/ (c) Side view of a connection.

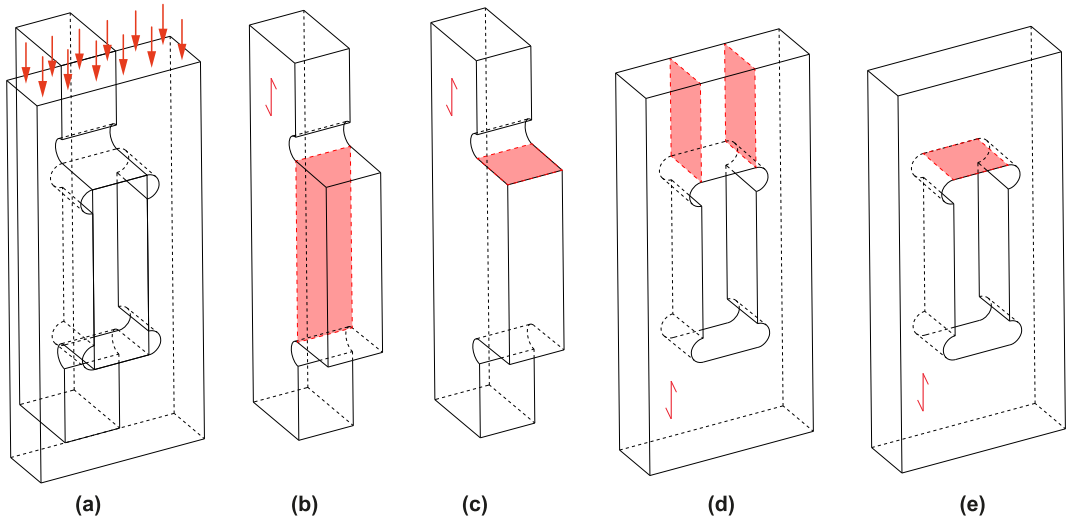

Fig. 2. Possible failure modes of a TT connection: (a) Axonometry of a TT joint loaded in its length direction/ (b) Shear failure area in tenon part/ (c) Compression failure area in tenon part/ (d) Shear failure area in mortise part/ (e) Compression failure area in mortise part.

using multiple TT joints in series [12] is used as reference for this investigation. It is designed for orthogonal prefabricated roof or slab components made of timber engineered panels. The different members can be single- or double-layered, as presented in Fig. 1a and b, depending on design choices and manufacturing possibilities. The grain orientation of different panels composing one element is always in the length direction and, as a result, parallel to the tenon length (Fig. 1c). The contours and TT joints of each panel are cut in a single operation with a CNC machine. This particular process creates notches, due to the cutting tool diameter, in the corners of TT joints both for the tenon (n_t) and the mortise (n_m). In addition to notches, TT joints are characterized by several geometrical parameters: the tenon length (l_t), the tenon thickness (t_t), the tenon height or mortise thickness (t_m), the tenon spacing (s_t), and a possible angle (α_t) to ease the assembly process. Different failure modes can be expected depending on these parameters when the connection is loaded in the length direction as shown in Fig. 2: (b) shear failure in the tenon, (c) compression failure in the tenon, (d) shear failure in the mortise, (e) compression failure in the mortise. Only shear and compression failures are of interest, since only tenons with a width-to-length ratio (t_m/l_t) less than or equal to one are studied here. If the slenderness of the tenon is higher than one, the failure modes could differ from those mentioned. This research investigates the shear failure in the tenon part (b) and the compression failures in both the tenon (c) and mortise (e) parts. The shear mortise failure (d) is not studied, as it can be easily avoided with basic geometrical considerations described in Eq. (1), where f_{vk} is the characteristic shear strength of the material. This equation can be simplified with Eq. (2) if the mortise and tenon part have the same thickness and material property. In most of the cases, the spacing between the tenons (s_t) is longer than the tenon length (l_t) and a shear failure of the mortise part rarely occurs.

$$f_{v,k,mortise} \times 2 \times s_t \times t_m > f_{v,k,tenon} \times l_t \times t_t \quad (1)$$

$$2s_t > l_t \quad (2)$$

Based on these considerations, there are several objectives in this paper: (i) determine the shear and compression load-carrying capacity of TT joints for different commonly available timber engineered panels and tenon lengths (l_t), (ii) calculate the estimated load-carrying capacity of TT joints according to existing European building standards (Eurocode 5 [13]) with the characteristic values given by the panel manufacturer's product specifications, and (iii) compare these design guidelines to the tests. For this purpose, an experimental campaign is performed with two different test setups especially developed to study the compression and shear behavior of TT connections. The test results are then compared to design criteria derived from standards and research.

2. Literature review

2.1. Design guidelines for wood-wood connections

Connections have a large influence on the structural performance of timber structures. Their mechanical behavior is an important parameter both for the serviceability limit state with their stiffness and for the ultimate limit state with their load-carrying capacity. The introduction of connection stiffness, called slip modulus (K_{ser}), was a major advance in the European standard Eurocode 5 (EC5) to solve problems of stability and large displacements, but it was only defined for steel fasteners such as nails, dowels, bolts, or screws. However, for the load-carrying

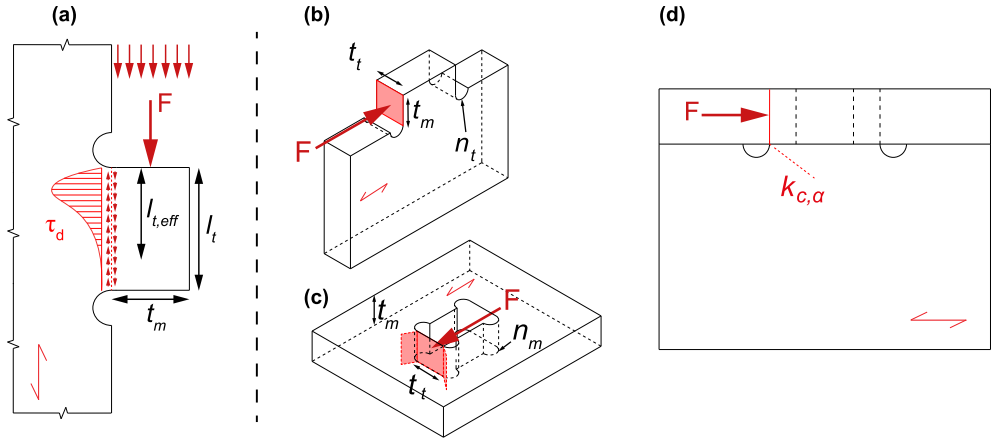

Fig. 3. Failure modes studied: (a) Shear failure in tenon part/ (b) Compression failure in tenon part/ (c) Compression failure in mortise part/ (d) Expected compression spreading in tenon part.

capacity of wood-wood connections, few guidelines are proposed in the Swiss standard [14] and in the national application document of German standard [15], although it is exclusively for traditional carpentry joints. Several research works are also performed on traditional joints, as it is an area of interest in the field of Built Heritage Restoration for the assessment and restoration of old timber constructions. Investigations on the strengthening of traditional carpentry joints [16,17] have been performed and on traditional as well as on tenon-mortise connections [18–20]. Unfortunately, these traditional joints are mainly for beam and post connections, and they are different from modern ones used for timber engineered panels. Nonetheless, a multiple tenons joint produced by CNC machines was studied by Claus et al. [21] but still for beam and post assembly. For timber plate products, new timber to timber contact joints were developed to reconstitute the diaphragm effect of cross laminated timber in modern structures [22–25]. Based on EC5 and these works, the failures of connections are generally verified with design equations, which can serve as a basis for the structural design of TT connections.

For the shear failure of the tenon part, more precisely presented in Fig. 3a, a, a non-uniform stress distribution called the Hammock Shape Shear Stress Distribution (HSSSD) can be expected according to several studies [26,27]. The design Eq. (3) can then be used:

$$\tau_d \leqslant k_{v,red} \times f_{v,k} \frac{k_{mod}}{\gamma_M} \tag{3}$$

$$\tau_d = \frac{F}{l_t \times t_t} \tag{4}$$

where τ_d is the design shear stress, $k_{v,red}$ is the coefficient for taking into account the non uniform shear stress distribution HSSSD, $f_{v,k}$ is the characteristic shear strength, k_{mod} is the modification factor for load duration and moisture content, and γ_M is the partial factor according to material properties.

For the compression failure, the different parameters are shown in Fig. 3d. A spreading of the compression strength can be expected according to EC5 and Verbist et al. [27]. It is taken into consideration with the coefficient ($k_{c,\alpha}$). The angle (α) is equal to 0 for the studied case as the grain orientation is always parallel to the joint length. The design Eq. (5) can therefore be used as reference:

$$\sigma_{c,d} \leqslant k_{c,\alpha} \times f_{c,0,k} \frac{k_{mod}}{\gamma_M} \tag{5}$$

$$\sigma_{c,d} = \frac{F}{t_t \times t_m} \tag{6}$$

$$k_{c,\alpha} = 1 + \sin\alpha \times (k_{c,90} - 1) \tag{7}$$

where $\sigma_{c,d}$ is the design compression stress, $f_{c,0,k}$ is the characteristic compression strength parallel to the grain, $k_{c,\alpha}$ represents the spreading of compression stress, and $k_{c,90}$ represents the spreading of compression stress perpendicular to the grain. The compression spreading in the mortise area is expected to be higher than the one in the tenon, as the stress can propagate on both sides of the tenon as shown in Fig. 3he same material properties, the compression failure should therefore happen in the tenon part.

2.2. Experimental protocols for the shear behavior of timber

Mostly related to the characterization of glued products like glued laminated timber (GLT) or cross laminated timber (CLT), there are several methods to characterize the shear properties of wood material in the literature in contrast to compression properties where the same method is generally used. For structural timber and GLT, the standard EN 408 [28] proposes to determine the shear strength parallel to the grain with an inclined setup as shown in Fig. 4a. Schmidt et al. [22,23] have used this typology of test setup for timber shear key connectors. It is a simple and efficient method to avoid expensive and time consuming steel setup but difficult to apply with the geometry of TT. For CLT, EN 16351 [29] introduces three methods: a basic one in annex D to determine shear strength f_v (Fig. 4c), an alternative one in annex F.3.3 to determine rolling shear strength and stiffness (Fig. 4b), and one inspired by an inclined setup in section F.4.2 to determine shear values within a layer (net cross section). For wood based panels, EN 789 [30] gives a method to determine panel shear properties with a particular loading arrangement as presented in (Fig. 4d). For planar shear properties a similar setup as the one shown in Fig. 4d is also presented but with glued steel plates on the side of panels. Finally, NF B51-032 [31], an old French standard published in 1981, presents a method for compressive shear test (Fig. 4e). Even though these different methodologies are complicated to be transposed directly to wood-wood connections as they are generally used for material specifications, they can inspire new experimental protocols. Push-out tests are also commonly used to study the shear behavior of timber joints [25]. Recently, specific investigations on TT joints related to two case-studies were performed with push-out tests [12,32]. These tests are convenient to use because they do not require any additional steel members for the setup. However, this method cannot be performed on a single joint. In 2016, a steel based setup was developed by Mira et al. [33] to investigate the shear behavior of digitally produced wood-wood connections, although the assembly geometry was different. Based on this work and the standard EN 789 [30], a new experimental setup for has been developed to investigate the shear behavior of TT.

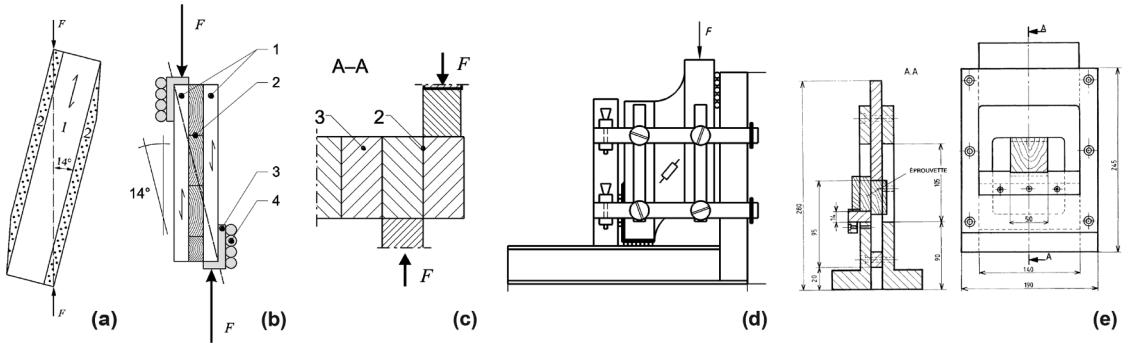

Fig. 4. Shear experimental setup for timber: (a) EN 408 [28]/ (b) EN 16351 Annex F.3.3 [29]/ (c) EN 16351 Annex D [29]/ (d) EN 789 [30]/ (e) NF B51-032 [31].

3. Material

This study was conducted on different types of timber engineered panels. They were chosen for their wide distribution among wood suppliers on the European market. Spruce oriented strand board type 3 (OSB 3), spruce as well as beech laminated veneer lumber (LVL), and spruce multiply solid wood (MSW) panels were investigated. A thin thickness of less than 40 mm was preferred considering the type of construction system developed using TT. Ongoing research on specific case-studies [7,12] have also influenced the choice of materials and thicknesses. The different panels are shown in Fig. 5 and their characteristics are listed in Table 1. Material properties and characteristics were obtained from: the standard EN 12369 [34] for OSB type 3 (Kronospan, Jihlava, Czech Republic), the VTT certificate [35] for spruce LVL Kerto Q®(Metsä Wood, Espoo, Finland), and the supplier technical certificate for beech LVL Baubuche Q®(Pollmeier, Creuzburg, Germany) [36] and spruce MSW (Dold®, Buchenbach, Germany) [37]. The density was determined at a relative humidity of 65 ± 5% and a temperature of 20 ± 2°according to EN 323 [38] (see Table A.8 in Appendix A). The tested material densities were approximately similar to the manufacturer's values, with the highest difference of only 5.26%. All the specimen types in this study were produced from different panels randomly selected in a batch of 10 panels per material to have a good statistical representation.

4. Compression behavior

The compression failure of TT connections was studied in two steps. First, the characteristic compression strength ($f_{c,0,k}$) was tested for each panel to determine a precise value ($f_{c,0,k,test}$) and to compare manufacturer's and test values. Second, the characteristic compression strength for TT connections ($\sigma_{c,k,TT}$) was determined experimentally. The 5% fractile values of the maximum load ($F_{max,0.05}$) were used to compare directly the compression strength ($\sigma_{c,k,TT}$) with the characteristic compression strength ($f_{c,0,k}$ and $f_{c,0,k,test}$) according to Eq. (8) and (9):

$$\sigma_{c,k,TT} = \frac{F_{max,0.05}}{t_t \times t_m} \tag{8}$$

$$\sigma_{c,k,TT} \leqslant k_{c,\alpha} \times f_{c,0,k} \tag{9}$$

with the compression spreading coefficient ($k_{c,\alpha}$) always equal to 1 as the grain orientation is parallel to the joint length. Eq. (9) is derived from Eq. (5) where the modification factor (k_{mod}) and partial factor (γ_M) were removed, as only 5% fractile characteristic values were directly compared. In addition, all the experimental data presented in this section is available in this open access data repository [47].

4.1. Material compression characterization

4.1.1. Method

Material compression tests were performed according to the standard EN 789 [30], which is used for the determination of mechanical properties for wood based panels. In B, the dimensions of each specimen type are listed in Table B.9 and the test setup is presented in Fig. B.13. A static universal testing machine (model LFV-200, Walter + Bai AG, Löhningen, Switzerland [39]) with a maximum loading capacity of 200 kN was used for the material specimens (1) (1') (2) (5) while another static machine (model PL 2.5 K, Schenck) with a maximum capacity of 2500 kN was used for (3) (4). The load was directly applied on the axis of the specimen top faces with a constant speed rate of 0.19 kN/s for (1), 0.24 kN/s for (1'), 0.27 kN/s for (2), 0.7 kN/s for (3), 0.1.5 kN/s for (4), and 0.3 kN/s for (5). A total number of 10 replicates per material were tested and two linear variable differential transformers (LVDT) were positioned on each side of the specimens.

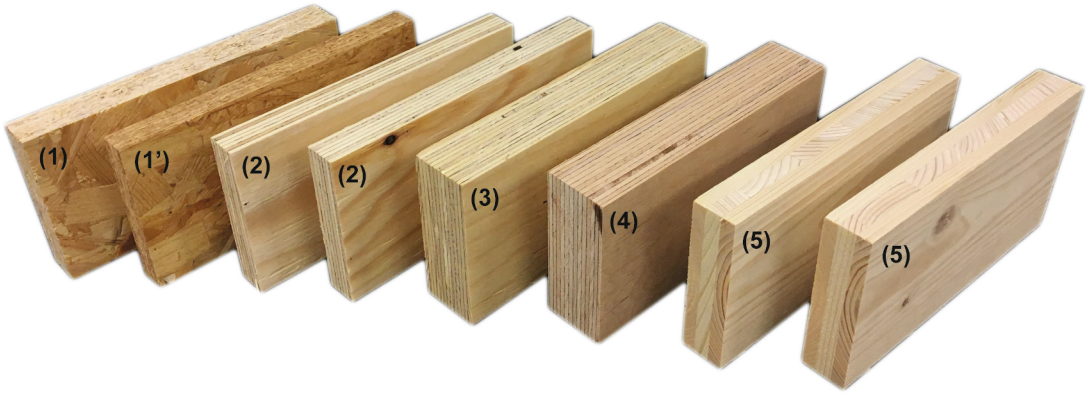

Fig. 5. Materials used for the experimental investigation on TT connections: (1) OSB type 3 25 mm/ (1') OSB type 3 18 mm/ (2) Spruce LVL 21 mm/ (3) Spruce LVL 39 mm/ (4) Beech LVL 40 mm/ (5) Spruce MSW 27 mm.

Table 1
Material properties for the experimental investigation on TT connections.

ID	Type –	Species –	Thickness (mm)	Plies number –	Lay-up –	Lay-up thickness (mm)	Thickness tolerance (mm)
(1)	OSB 3	Spruce	25	3	| – |	–	+ − 0.8
(1')	OSB 3	Spruce	18	3	| – |	–	+ − 0.8
(2)	LVL	Spruce	21	7	| – ||| – |	3 each	−1.03 + 1.43
(3)	LVL	Spruce	39	13	|| – ||| – ||| – ||	3 each	−1.57 + 1.97
(4)	LVL	Beech	40	14	||| – ||||| – |||	3 each*	+ − 1
(5)	MSW	Spruce	27	3	| – |	6.9/13.2/6.9	+ − 1

* 2 mm on the 2 outer layers because of the finishing process.

4.1.2. Results

The average ultimate load (F_{max}) was determined from the tests. The 5% fractile value ($F_{max,0.05}$) was then calculated in order to compare the tested characteristic compression strength ($f_{c,0,k,test}$) with the characteristic strength given by panel manufacturers ($f_{c,0,k}$). The methodology for calculating the 5% fractile values ($F_{max,0.05}$) is presented in Appendix B.2. All the results are summarized in Table 2.

For OSB 25 and 18 mm, $f_{c,0,k,test}$ was significantly lower than $f_{c,0,k}$ with a difference of −34.49% and −37.92% respectively. On the opposite, $f_{c,0,k,test}$ for spruce LVL 21 mm and spruce MSW 27 mm was significantly higher than $f_{c,0,k}$ with a difference of 41.67% and 74.59% respectively. Concerning spruce LVL 39 mm and beech LVL 40 mm, the values of $f_{c,0,k,test}$ were the closest to $f_{c,0,k}$ with a difference of only 11.83% and 3.55% respectively. The significant differences in the results, whether negative or positive, have emphasized the variability between standard and test values depending on the panel type. The test values, $f_{c,0,k,test}$, were thus used to investigate the compression behavior of the TT connections and estimate if a compression spreading occurs or not. In addition, the characteristic values, $f_{c,0,k}$, were also used for comparison with the standard guidelines.

Table 2
Results of compression tests per material according to EN 789 [30].

ID	F_{max} (kN)	$c_{v,\mathrm{Fmax}}$ (%)	$F_{max,0.05}$ (kN)	Section (mm^2)	$f_{c,0,k,test}$ (MPa)	$f_{c,0,k}$ (MPa)	δ (%)
(1)	41.82	7.02	36.50	3618	10.09	15.40	−34.49
(1')	53.78	7.81	45.94	5000	9.19	14.80	−37.92
(2)	120.10	3.15	113.05	4200	26.92	19.00	41.67
(3)	237.24	2.36	226.80	7800	29.08	26.00	11.83
(4)	460.84	2.28	441.55	8000	55.19	53.30	3.55
(5)	118.75	4.78	108.42	5400	20.08	11.50	74.59

4.2. Experimental setup

The compression behavior of the TT joints was investigated with an experimental setup presented in Fig. 6. The same static universal testing machine [39], presented in Section 4.1.1, with a maximum loading capacity of 200 kN was used. Loads were applied in the joint axis and two 10 mm thick steel plates (6)(9) were used to avoid local indentation at the top and bottom faces of the specimens. Lateral restraints (3) were positioned to prevent a lateral shift of the sample with respect to the loading axis. A support plate (4) was bolted to the testing machine. Beech LVL was chosen to compose the setup for its high mechanical characteristics. Two LVDTs were placed on each side of the samples to record the relative displacement at the contact area (d). The standard EN 26891 [40] gives the general principles for the determination of strength and deformation characteristics for joints made with mechanical fasteners. Since it is a very close topic, the loading procedure described in EN 26891 was followed for these tests.

4.3. Specimens

The specimen geometries are described in Fig. 7 and all the properties are listed in Table 3. According to the possibilities of the construction system, single- and double-layered (SL and DL, respectively) TT joints were studied. The materials described in Section 3 were assembled as follow: OSB 3 18 and 25 mm (DL), spruce LVL 21 mm (DL), spruce LVL 39 mm (SL), beech LVL 40 mm (SL) and spruce MSW 27 mm (DL). Only TT joints made of the same material were studied. The influence of different material combinations could be investigated in future research. The design objective was to reach the compression limit of the TT assembly for one connection. The geometry was thus carefully designed to prevent a shear failure, since the tenon length (l_t) can be considered infinite (see Fig. 7b). The grey part of the specimen represented the TT connection, while the other part was only manufactured to prevent a lateral displacement of the mortise part. The parameter e_t was kept as small as possible to avoid additional friction in the experimental setup and $l_{t,2}$ was minimized even though a certain distance is necessary for the overall stability of the setup. The mortise part, shown in Fig. 7d, was a basic mortise geometry cut in its cross-sectional plane. With this configuration, the load was applied directly on the top face of the mortise part to study the compression behavior. The dimensions were chosen for the scale of one TT joint according to the panel thicknesses studied. All the tests were performed with the grain orientation parallel to the joint length. A total of 15 replicates per specimen type were produced with a CNC machine. A spiral router cutter Marathon (ID 240502, Leitz®, Oberkochen, Germany [41]) was used with a diameter of 12 mm, a rotational speed of 18 000 rpm, and a feed speed of 4.5 m/min. The notch diameters n_t and n_m were 13 mm as fixed parameters for all specimens due to the cutting tool diameter of 12 mm. The tool diameter was a good compromise to minimize the loss of material in the assembly area and to keep a tool strong enough for an efficient production (number of machining cycles, tool wear). It was already a relatively small-sized tool compared to those used in timber construction. No additional gaps were added during the contouring of the TT joints. Finally, the material and samples were conditioned in a normalized environment with a temperature of 20°C and relative humidity of 65% [42].

4.4. Results

All the results of the compression tests for TT joints are listed in Table 4 and the failures per specimen type are shown in Fig. 8. The load–displacement curves and the statistical distribution can be found in C (see Fig. C.14). The coefficients of variation for the maximum loads (F_{max}) were quite low with a maximum value of 6.75%. The experimental procedure is thus consistent for this type of tests.

Due to the variability between the characteristic compression properties and real performance of materials emphasized in Section 4.1.2, significant differences were observed between the compression strengths $\sigma_{c,k,TT}$ and $f_{c,0,k}$. For OSB TT joint (EM1), $\sigma_{c,k,TT}$ was 22.09% lower than $f_{c,0,k}$, while it was 47.79% and 82.70% higher for spruce LVL

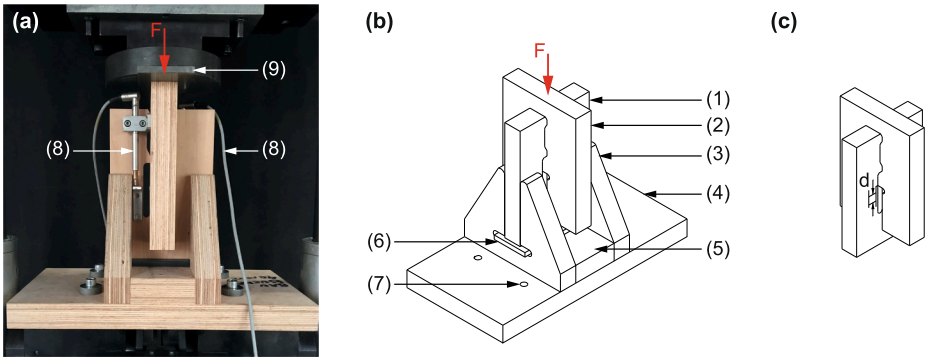

Fig. 6. Compression experimental setup for TT connections: (a) Side view: (8) two LVDTs sensors, (9) Steel plate 10 mm/ (b) Technical axonometry: (1) Tenon part of the specimen, (2) Mortise part of the specimen, (3) Lateral restraints, (4) Support plate (5) Support plate, (6) Steel plate 10 mm, (7) Bolt ∅24 mm/ (c) Specimen: *d* is the measured area.

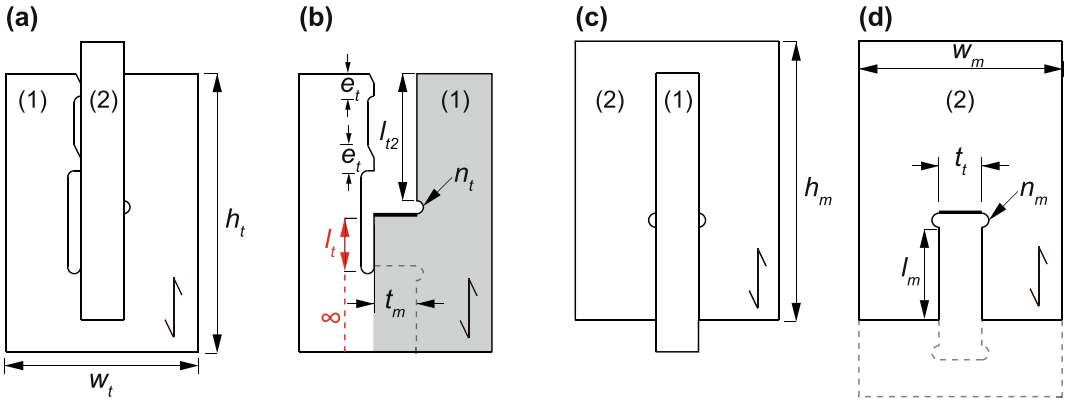

Fig. 7. TT compression specimens: (1) Tenon part, (2) Mortise part/ (a) Face view/ (b) Face view with only (1), the grey part represents the TT connection/ (c) Side view/ (d) Side view with only (2).

(EM2) and MSW (EM5) respectively. Therefore, EC5 guidelines defined by Eq. (9) were either largely underestimating or overestimating the real load-carrying capacity, placing EM1 on the unsafe side of design for example. For the single-layered joints EM3 and EM4, the difference were less pronounced as their compression properties were more precisely determined. The material characterization announced by panel manufacturers $f_{c,0,k}$ plays a major role to correctly calculate the compression strength of TT.

On the other hand, $\sigma_{c,k,TT}$ was 10.84% higher in average for all the materials than the real compression performance $f_{c,0,k,test}$, with differences ranging from 4.32% to 25.50%. The value of EM1 was approximately 25% higher while the values of the specimens EM2, EM3, EM4 and EM5 were only 7% higher in average. The internal panel lay-up and the material variability influence this phenomenon. Thus, these results highlight a compression spreading only in the OSB TT joints (EM1). The spreading coefficient $k_{c,\alpha}$ equal to 1 with the grain orientation parallel to the joint (Eq. (9)) is thus consistent when compared to the results obtained on the other materials. However, considering the high variability between $f_{c,0,k}$ and $f_{c,0,k,test}$ for several panels (EM1, EM2 and EM5), it is difficult to establish a general rule for the compression spreading coefficient for TT connections made of timber engineered panels. A recommended spreading coefficient $k_{c,\alpha}$ could be defined according to the material type and joint geometry if the product specifications of the material are accurate. Otherwise, it is on the safe side of design to not consider the spreading.

Table 3
Specimen properties for compression tests on TT as described in Fig. 7.

ID	EM1	EM2	EM3	EM4	EM5
Materials	OSB3	Kerto Q	Kerto Q	Baubuche	MSW
Layers	2	2	1	1	2
h_t (mm)	260	260	260	260	260
w_t (mm)	180	180	180	180	180
t_t (mm)	50	42	39	40	54
l_t (mm)	50	50	50	50	50
$l_{t,2}$ (mm)	117	117	117	117	117
e_t (mm)	10	10	10	10	10
h_m (mm)	260	260	260	260	260
w_m (mm)	190	190	190	190	190
t_m (mm)	36	42	39	40	54
l_m (mm)	87	87	87	87	87

5. Shear behavior

For the shear behavior of TT connections, the characteristic shear strength ($f_{v,k}$) of each material was not tested. Manufacturer's values were used directly for this investigation, as the variability between product specifications and real performance was already highlighted by material compression tests. The shear strength of TT ($\tau_{v,k,TT}$) was

Table 4
Results of compression tests on TT connections per specimen type.

Designation	Units	EM1	EM2	EM3	EM4	EM5
F_{max}	(kN)	22.72	54.84	51.14	106.83	67.70
$c_{v,\mathrm{Fmax}}$	(%)	6.55	5.47	5.11	3.89	6.75
$F_{max,0.05}$	(kN)	20.77	49.55	47.48	99.28	61.24
Section	(mm^2)	1800	1764	1521	1600	2916
$\sigma_{c,k,TT}$	(MPa)	11.53	28.08	31.21	62.05	21.01
$\delta_{\sigma_{c,k,TT}//f_{c,0,k}}$	(%)	−22.09*	47.79	20.04	16.36	82.70
$\delta_{\sigma_{c,k,TT}//f_{c,0,k,test}}$	(%)	25.50*	4.32	7.34	12.42	4.64

* Reference: OSB 18 mm as it has the lowest $f_{c,0,k,test}$.

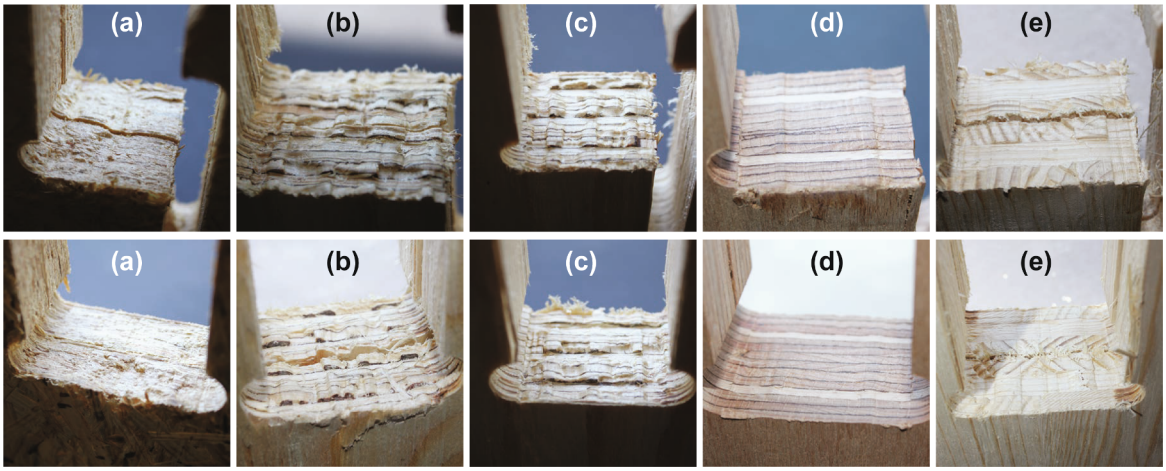

Fig. 8. Failure pictures of all TT specimens in compression: (a) EM1/ (b) EM2/ (c) EM3/ (d) EM4/ (e) EM5.

defined according to Eq. (10) with the 5% fractile values ($F_{max,0.05}$) extracted from the tests. The EC5 guideline based on Eq. (3) and defined by Eq. (11) was used for comparison. In a first approach, the reduction coefficient ($k_{v,red}$) was considered equal to 1 and the modification factor (k_{mod}) and partial factor (γ_M) were removed, as only 5% fractile characteristic values were directly compared.

$$\tau_{v,k,TT} = \frac{F_{max,0.05}}{l_t \times t_t} \tag{10}$$

$$\tau_{v,k,TT} \leqslant k_{v,red} \times f_{v,k} \tag{11}$$

5.1. Experimental setup

An experimental setup was developed to perform shear tests on single TT joint as shown in Fig. 9a. All the details are presented on a technical drawing and a schematic drawing in Fig. 9b and c. Specimens were positioned in a rigid steel frame anchored inside a static universal testing machine with a maximum loading capacity of 200 kN [39]. The hydraulic jack applied pressure on the axis of the mortise specimen (4) through a steel plate of 40 mm thickness (1) possessing the same dimensions as the mortise specimen to avoid local indentation. The tenon specimen (5) was rigidly fixed on its top by a steel plate of 15 mm thickness (3) and four bolts of 24 mm diameter (2), two on each side. A 5 mm thick steel plate (6) was welded to the lower part of the bolts to keep them into their initial position and avoid lateral displacements. In addition, a 40 mm thick beech LVL plate (7) was bolted to the setup to maintain in position and prevent the rotation of the lower part of the tenon specimen. The mortise specimen was kept in position thanks to the 20 mm thick steel plate (8) and the steel bracket (11). They were fastened with eight bolts of 12 mm diameter. Two other bolts of 12 mm diameter (9) linked the steel plates (8) and (3) on each side of the mortise specimen to stiffen the lateral displacement of the setup. Two Teflon plates (10) were positioned between the steel plate (8) and the mortise specimen to remove friction between these parts. Two LVDTs were mounted on each side of the specimens at the axis of the TT (12). The lateral displacement of the setup was verified with 4 LVDTS positioned on plate (3) and (8) and it was negligible. The loading protocol described in EN 26891 [40] was also used as for the compression tests on TT joints.

5.2. Specimens

The specimen geometries are displayed in Fig. 10 and all the properties are listed in Table 5. The same material and layer configurations were used as those described for compression tests in Section 4.3. For all the materials, tenon lengths (l_t) of 50, 100, and 150 mm were considered except for OSB 3 where they were equal to 50, 65, and 80 mm due to its low compression strength. Eq. (2) was respected for each specimen to determine the height (h_m) and avoid a shear failure in the mortise specimen. The height (h_t) was then established by adding 20 mm for displacements during the tests. The widths of the mortise (w_m) and tenon (w_t) were calculated to be respectively at least 3 times larger than the tenon thickness (t_t) and mortise thickness (t_m). An insertion angle (α_t) of 1°was defined to ease the insertion of the tenon in the mortise as each panel has a thickness tolerance (see Table 1), which can make the assembly process difficult. All the tests were performed

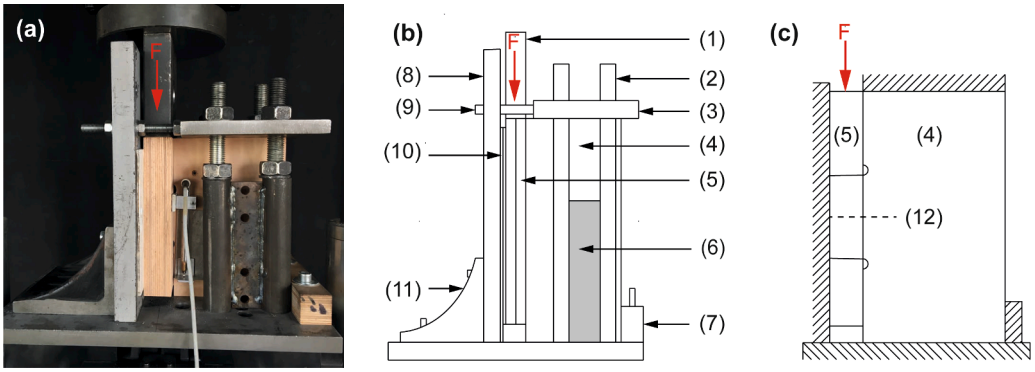

Fig. 9. Side view of the shear experimental setup for TT connections: (a) Photograph/ (b) Technical drawing: (1) Steel plate 40 mm, (2) Bolt ∅24 mm, (3) Steel plate 15 mm, (4) Specimen with tenon, (5) Specimen with mortise, (6) Steel plate 5 mm, (7) Beech LVL 40 mm, (8) Steel plate 20 mm, (9) Bolt ∅12 mm, (10) Two Teflon plates, (11) Steel bracket 20 mm with 8 bolts ∅12 mm/ (c) Schematic drawing: (12) Two LVDTs sensors.

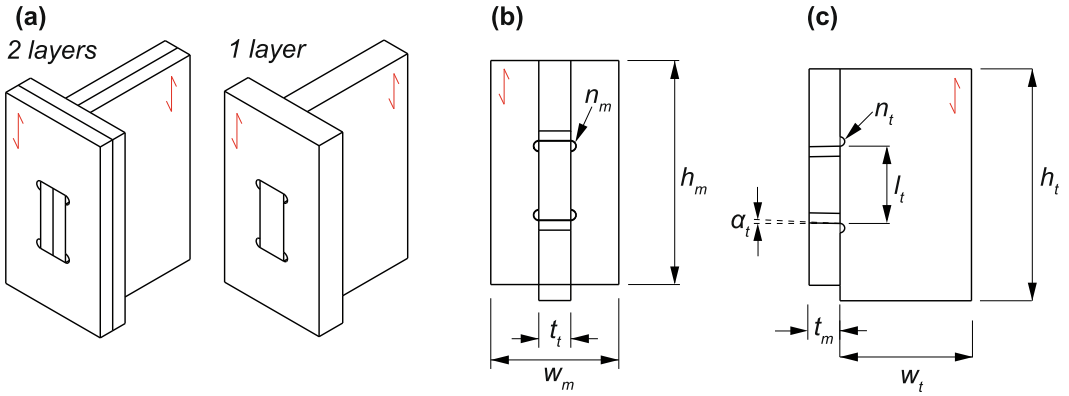

Fig. 10. TT shear specimens: (a) Axonometries of single- and double-layered type/ (b) Front view/ (c) Side view.

with the grain orientation parallel to the joint length. A total of 20 replicates per specimen type were produced with a CNC machine and the same manufacturing parameters described in Section 4.3. The material and samples were also conditioned in a normalized environment with a temperature of 20°C and relative humidity of 65% [42].

5.3. Results

All the results of the shear tests on TT connections are listed in Table 6 and the failure pictures are displayed in Fig. 11. The load displacement curves as well as the statistical distribution of the maximum load (F_{max}) per specimen type can be found in D (see Fig. D.15–D.20). The maximum load variability was acceptable for all the tests ranging from 3.67% to 9.89% and showing the good consistency of the experimental procedure. All the experimental data is available in this open access data repository [47].

Concerning the OSB connections (T1), a compression failure happened instead of a shear failure in the specimens with the maximum tenon length (T1-80) because of the significant difference between $f_{c,0,k}$ and $f_{c,0,k,test}$ (see Fig. 11a'). The specimens T1-80 were thus discarded from the analysis of the shear behavior. On the other hand, a shear failure occurred for the specimens T1-50 and T1-65 as expected (see Fig. 11a). The shear strength $\tau_{v,k,TT}$ for T1-50 and T1-65 was respectively 27.08% and 21.84% lower than $f_{v,k}$. The difference could also be explained by the variability between the announced characteristic strength and real performance of the material. However, if the reduction coefficient $k_{v,red}$ is applied with a value of 0.8, as described in national application documents of EC5 [27], $\tau_{v,k,TT}$ is only 5.62% lower than $f_{v,k}$ on average for the two tenon lengths. On the opposite, $\tau_{v,k,TT}$ for spruce MSW (T5) was significantly higher than $f_{v,k}$ with a difference of 124.42%, 111.52%, and 120.53% for the three different tenon

Table 6
Results of shear tests on TT connections per specimen type.

ID	F_{max} (kN)	$c_{v,F_{max}}$ (%)	$F_{max,0.05}$ (kN)	Section (mm^2)	$\tau_{v,k,TT}$ (MPa)	$f_{v,k}$ (MPa)	$\delta_{\tau_{v,k,TT}//f_{v,k}}$ (%)
T1-50	14.30	7.16	12.58	2500	5.03	6.90	−27.08
T1-65	19.09	5.52	17.53	3250	5.39	6.90	−21.84
T1-80	21.13	6.06	19.01	4000	4.75	6.90	−31.12
T2-50	13.52	8.12	11.69	2100	5.57	4.50	23.68
T2-100	27.58	7.17	23.83	4200	5.67	4.50	26.06
T2-150	40.77	5.16	37.18	6300	5.90	4.50	31.14
T3-50	11.57	8.52	10.07	1950	5.16	4.50	14.73
T3-100	22.90	7.18	19.97	3900	5.12	4.50	13.80
T3-150	34.43	5.31	30.89	5850	5.28	4.50	17.34
T4-50	23.66	3.67	22.19	2000	11.09	7.80	42.23
T4-100	47.99	7.38	41.79	4000	10.45	7.80	33.96
T4-150	68.03	6.98	59.35	6000	9.89	7.80	26.81
T5-50	19.14	9.89	16.36	2700	6.06	2.70	124.42
T5-100	35.17	6.27	30.84	5400	5.71	2.70	111.52
T5-150	53.61	6.49	48.23	8100	5.95	2.70	120.53

Table 5
Specimen properties for shear tests on TT as described in Fig. 10.

ID	Materials	Layers	l_t (mm)	h_t (mm)	h_m (mm)	w_t (mm)	w_m (mm)	t_t (mm)	t_m (mm)
T1-50	OSB 3	2	50	250	230	163	156	50	36
T1-65	OSB 3	2	65	250	230	163	156	50	36
T1-80	OSB 3	2	80	250	230	163	156	50	36
T2-50	Spruce LVL	2	50	250	230	169	160	42	42
T2-100	Spruce LVL	2	100	300	280	169	160	42	42
T2-150	Spruce LVL	2	150	350	330	169	160	42	42
T3-50	Spruce LVL	1	50	250	230	169	160	39	39
T3-100	Spruce LVL	1	100	300	280	169	160	39	39
T3-150	Spruce LVL	1	150	350	330	169	160	39	39
T4-50	Beech LVL	1	50	250	230	169	160	40	40
T4-100	Beech LVL	1	100	300	280	169	160	40	40
T4-150	Beech LVL	1	150	350	330	169	160	40	40
T5-50	Spruce MSW	2	50	250	230	169	160	54	54
T5-100	Spruce MSW	2	100	300	280	169	160	54	54
T5-150	Spruce MSW	2	150	350	330	169	160	54	54

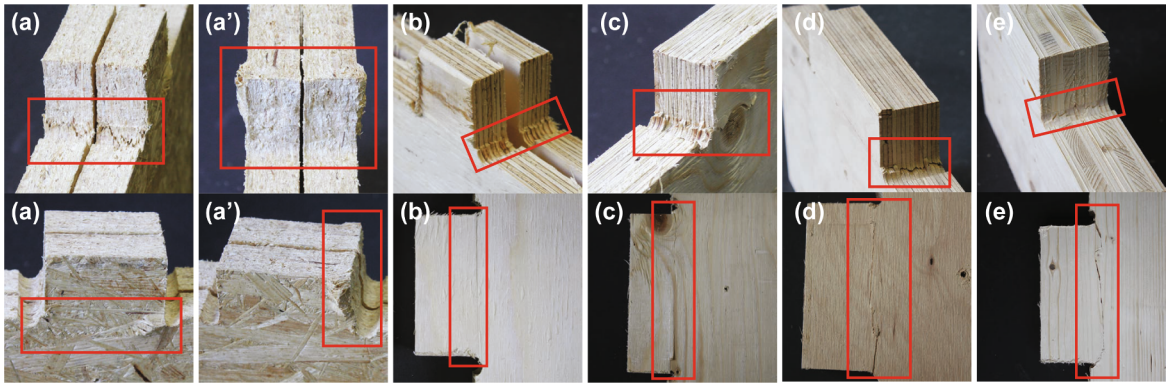

Fig. 11. Shear failure pictures: (a) T1-50/ (a') T1-80/ (b) T2/ (c) T3/ (d) T4/ (e) T5.

lengths. The material characterization showed large differences for the compression strength and could explain partially these differences for T1 and T5. These two panels have a particular lay-up described in Table 1 with a large cross-layer in the middle, which could also play a role in these differences between announced material characteristics and their real performances.

For LVL specimens T2 and T3, a clear shear failure occurred in the expected area of the joints as shown in Fig. 11b and c. Nonetheless, the differences between $\tau_{v,k,TT}$ and $f_{v,k}$ were 25% for T2, while only 15% for T3 on average for the three different tenon lengths. The number of layers of the TT joint could thus influence its resistance. The resistance for shorter tenon lengths was highlighted for spruce LVL T2 and T3 whereas the opposite was observed for beech LVL T4. On average for T4, $\tau_{v,k,TT}$ was approximately 35% higher than $f_{v,k}$ with a clear shear failure (see Fig. 11d). Globally, $\tau_{v,k,TT}$ for LVL panels was 25% higher than the EC5 guidelines defined by Eq. (11) without taking into consideration the reduction coefficient $k_{v,red}$. It seems that for the particular TT geometry and with accurate material characteristics, the reduction coefficient $k_{v,red}$ is not relevant. Moreover, a diffusion could be observed as the assembly strength is higher than the expected one. Additional tests on the shear properties of each panel should be performed to verify this possible phenomenon, since no material characterization of the shear properties was carried out in this study.

6. Discussions

A summary of the different test results is presented in this section. The load-carrying capacity of TT connections is defined by several failure modes as described in Fig. 2. Shear and compression failures, illustrated in Fig. 3vestigated and compared to EC5 guidelines in Sections 4.4 and 5.3. All the results are summarized in Table 7. In addition, the results for each specimen type are presented in a graph where the characteristic load ($F_{max,0.05}$) is function of the tenon length (l_t) as shown in Fig. 12. The area of interest is defined from a tenon length of 50 mm to the optimum tenon length determined when the resistant shear capacity reaches the compression capacity of the joint. The optimum tenon length was defined for both the tests ($l_{t,optim,test}$) and the EC5 guidelines ($l_{t,optim,EC5}$). The optimum length derived from EC5 can be calculated according to these equations (if $k_{v,red}$ and $k_{c,\alpha}$ are considered equal to 1):

$$f_{v,k} \times l_t \times t_t > f_{c,0,k} \times t_m \times t_t \tag{12}$$

$$l_{t,optim,EC5} > \frac{f_{c,0,k} \times t_m}{f_{v,k}} \tag{13}$$

The differences between $l_{t,optim,EC5}$ and $l_{t,optim,test}$ were between 2 to 15% approximately. Although, these values were relatively close for the different panels, the load-carrying capacities at this point were different depending on the panel type. In the analysis, it is assumed that only the shear load-carrying capacity is considered until the compression load-carrying capacity is reached. No strength coupling was investigated in a first approach.

Table 7
Summary of the test results for TT connections.

Designation	Units	T1&EM1	T2&EM2	T3&EM3	T4&EM4	T5&EM5
Materials	–	Spruce	Spruce	Spruce	Beech	Spruce
Type	–	OSB 3	LVL	LVL	LVL	MSW
TT layers	–	2	2	1	1	2
$f_{v,k}$	(MPa)	6.9	4.5	4.5	7.8	2.7
$\tau_{v,k,TT}$	(MPa)	5.21	5.71	5.19	10.48	5.91
$\delta_{\tau_{v,k,TT}//f_{v,k}}$	(%)	−24.46	26.96	15.29	34.33	118.82
$\sigma_{c,k,TT}$	(MPa)	11.53	28.08	31.21	62.05	21.01
$\delta_{\sigma_{c,k,TT}//f_{c,0,k}}$	(%)	−22.09	47.79	20.04	16.36	82.70
$\delta_{\sigma_{c,k,TT}//f_{c,0,k,test}}$	(%)	25.50	4.32	7.34	12.42	4.64
$l_{t,optim,EC5}$	(mm)	77.22	177.33	225.33	273.33	230.00
$l_{t,optim,test}$	(mm)	78.82	201.84	232.20	248.15	192.43
$\delta_{EC5//Test}$	(%)	2.07	13.82	3.05	-9.21	-16.33

To summarize, Only the load-carrying capacity of OSB TT joints (T1 &EM1) is overestimated by 25% according to EC5 (Fig. 12a). On the contrary, the load-carrying capacity of spruce MSW joints (T5&EM5) is largely underestimated by half (Fig. 12e). Both of these materials showed significant differences between the characteristic values announced by the manufacturer (or the material standard) and those tested. It is thus complicated to structurally design such connections without experiments because of this large variability. On the other hand, TT joints made of LVL panels are underestimated by approximately 25% with more precise material properties (Fig. 12b,c and d). The closest to EC5 guidelines was the single-layered spruce LVL connection (T3&EM3) with a difference of approximately 15%. Moreover, as the characteristic compression strength ($f_{c,0,k,test}$) was tested for all materials, a compression spreading of 25% was highlighted only for the OSB TT joints. The same value was observed for the shear strength of LVL panels, which could also demonstrate a spreading phenomenon for the shear behavior.

Among the developments towards a more comprehensive code on timber structures, Dietsch et al. [43] stated that the determination of shear properties of wood-based panels applied in structural design could be improved. They also mentioned three methods to develop standards for structural design: tabulated data or design diagrams, simplified design methods, and scientifically based design methods. They highlighted as well that design diagrams are useful methods for standard applications, which corresponds to the structural elements developed with TT connections [12]. Based on materials composing a TT assembly, different approaches could be determined. LVL panels

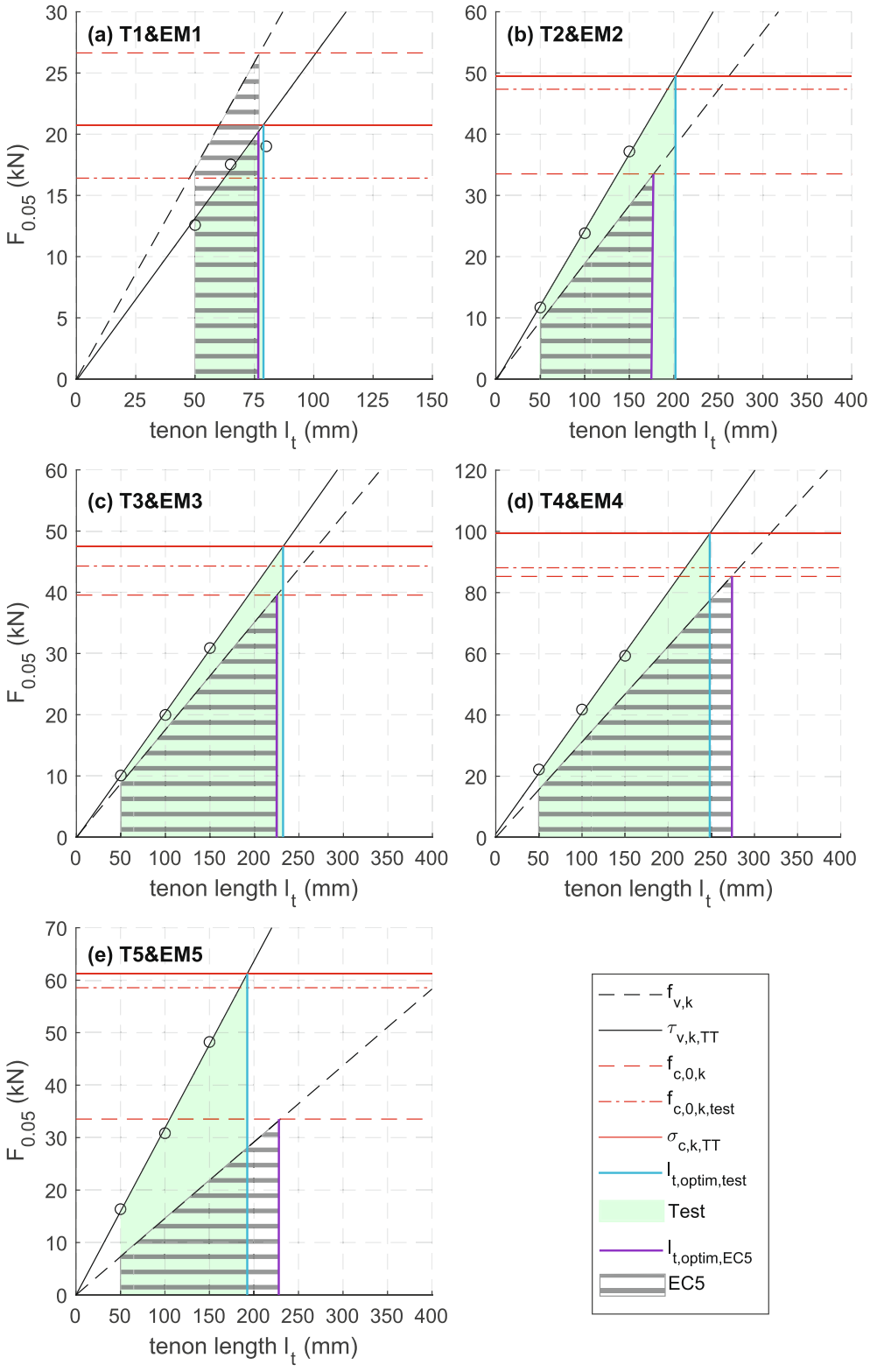

Fig. 12. load-carrying capacity of TT connections as function of tenon length.

could be designed with EC5 equations with research on spreading coefficients to optimize the TT connection, as they already have a good correlation between product specifications and characteristic values. Otherwise, design diagrams could be used for materials such as OSB and spruce MSW, which possess a higher variability between manufacturer specifications and characteristic values. These diagrams can be based on experimental tests following the procedures developed in Section 5.1 for shear and in 4.2 for compression. They can be inspired from Fig. 12 with different parameters such as material, tenon length, panel thickness, material lay-up and others, as they were shown to influence the TT behavior.

7. Conclusion

The in-plane load-carrying capacity of digitally produced through tenon (TT) joints was investigated in this paper, as they are increasingly applied for standard construction systems. Shear and compression failure modes were considered and two test setups were developed for this purpose. An experimental campaign was performed on commonly available timber panels to expand knowledge for several materials. The scope of the study was limited to a grain orientation parallel to the joint and three different tenon lengths. The experimental results were compared to existing Eurocode 5 (EC5) guidelines for traditional carpentry assemblies to assess the existing state of the art for the structural design of such joints.

First, significant differences were observed between the announced characteristic strength values and real performances of the materials, especially for OSB and MSW panels. The material characteristics are of high importance to determine accurately the load-carrying capacity through design criteria derived from EC5. This variability is thus problematic to perform a safe design with, for example, the overestimation of the OSB compression strength and probably the shear strength as well. It is less critical when the properties are overestimated such as for all the other materials, but it is not relevant for an optimized and coherent design. As it was stated by Dietsch et al. [43], the correlation between product specifications and EC5 could well be improved in general, and more particularly for the shear behavior of timber.

Second, existing EC5 guidelines were mainly on the safe side of design. Only the capacity of OSB TT joints was overestimated by 25% while all the others were underestimated. The highest difference was for the spruce MSW with twice the load-carrying capacity expected. These two materials (OSB and MSW) were characterized by a particular lay-up with a large cross-layer in the middle of the panels, which could have increased these differences. The closest to EC5 was the single-layered spruce LVL connection with a difference of only 15% while all the LVL specimens were underestimated by approximately 25% on average. Based on the tests results, a compression spreading of 25% was highlighted only for the OSB material. The EC5 compression spreading coefficient ($k_{c,\alpha}$) equal to 1 when the grain orientation is parallel to the joint is consistent, and contributes only for OSB panels to the underestimation of the load-carrying capacity of the joint if the material characteristics are accurately defined by tests.

The same phenomenon was observed for the shear strength of the LVL specimens. Therefore, a shear spreading could probably be considered instead of the reduction factor coefficient ($k_{v,red}$) defined in EC5 due to the non-uniform stress distribution of shear. However, additional tests on the shear material properties should be carried out to confirm this assumptions in future research. In addition, it is troublesome to define general guidelines for the use of spreading coefficient, as the TT behavior varies considerably depending on the material used.

Finally, different methods can be proposed for a convenient structural design of such wood-wood connections. If the product specifications are considered uncertain, as it was the case for OSB and MSW, design diagrams based on the experimental procedures developed in this work can be implemented. On the other hand, EC5 design criteria can be used when the product specifications are more precise such as for LVL panels. New optimized guidelines could be defined in future research with additional tests on the TT behavior and shear material characteristics.

CRediT authorship contribution statement

Julien Gamerro: Conceptualization, Methodology, Validation, Formal analysis, Investigation, Data curation, Writing - original draft, Visualization, Project administration. **Jean Francois Bocquet:** Conceptualization, Methodology, Validation, Formal analysis, Writing - review & editing, Supervision. **Yves Weinand:** Conceptualization, Writing - review & editing, Supervision, Funding acquisition.

Acknowledgments

The authors would like to thank Martin Nakad from the Laboratory for Timber Constructions (IBOIS, EPFL) for his valuable contribution to this work. The authors would also like to acknowledge the support and assistance of the Structural Engineering Group of EPFL. This research was supported by the NCCR Digital Fabrication, funded by the Swiss National Science Foundation (NCCR Digital Fabrication Agreement #51NF40-141853).

Appendix A. Material densities

See Table A.8

Table A.8
Measured material densities $\rho_{mean,test}$ compared to manufacturer's values ρ_{mean}.

ID	$\rho_{mean,test}$ (kg/m^3)	ρ_{mean} (kg/m^3)	δ_ρ (%)
(1)	605.29	600	0.88
(1')	595.92	600	−0.68
(2)	485.37	510	−4.83
(3)	483.18	510	−5.26
(4)	799.35	800	−0.08
(5)	462.03	480	−3.74

Appendix B. Material compression tests

B.1. Method and specimens

See Fig. B.13

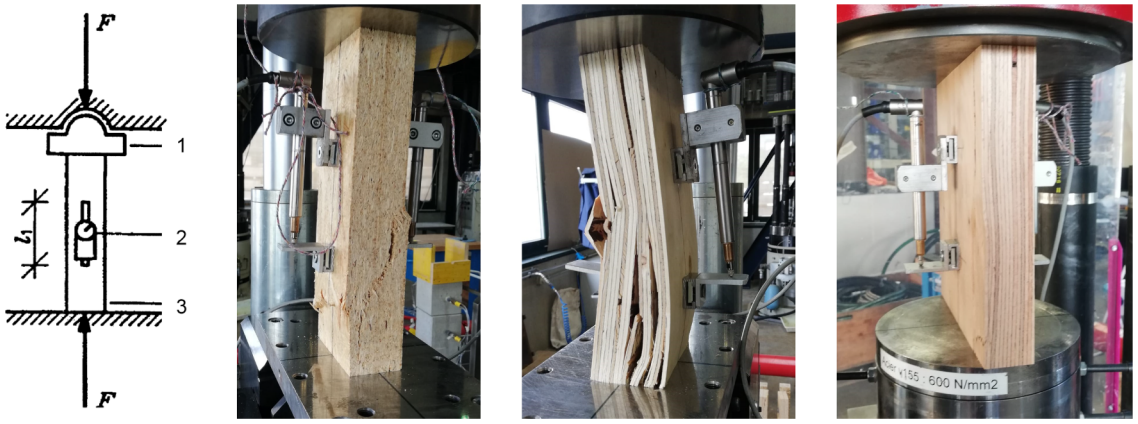

Fig. B.13. Compression setup: (a) EN789 [30] (1) Spherical seated (2) Transducer (3) Test piece/ (b) OSB specimen/ (c) Spruce LVL specimen/ (d) beech LVL specimen.

See Table B.9

Table B.9
Specimen properties for compression tests according to EN 789 [30].

ID	Material thickness (mm)	Number of layer (mm)	Total thickness (mm)	Width (mm)	Length (mm)
(1)	18	3	54	67	300
(1')	25	2	50	100	300
(2)	21	2	42	100	240
(3)	39	2	78	100	430
(4)	40	1	40	200	240
(5)	27	2	54	100	290

B.2. Methodology for calculating the 5% fractile values

The 5% fractile value ($F_{max,0.05}$) was determined according to the methodology defined in Annex D of Eurocode 0 [44]. The coefficient of variation ($c_{v,F_{max}}$) for each material was under 10%. As a result, a small sample size of 10 replicates is sufficient to determine the characteristic strength according Hunt et al. [45]. A log-normal distribution was assumed, which is generally the case for compression strength parallel to the grain for timber properties [46]. Eqs. (B.1)–(B.3) from Eurocode 0 were used:

$$F_{max,0.05} = exp[m_y - k_n s_y] \tag{B.1}$$

$$m_y = \frac{1}{n}\sum_{i=1}^{n} ln(F_{max,i}) \tag{B.2}$$

$$s_y = \sqrt{\frac{1}{n-1}\sum_{i=1}^{n} (ln(F_{max,i}) - m_y)^2} \tag{B.3}$$

where F_{max} is the maximum load, n is the number of specimens, k_n is the characteristic fractile factor for a sample size of 10 replicates (constant value of 1.92), m_y is the average of the natural logarithm values, and s_y is the standard deviation of the natural logarithm values. All the results are listed in Table B.10.

Table B.10
Test results of the maximum load (F_{max}) for the material compression tests.

Material ID Units	(1) (kN)	(1') (kN)	(2) (kN)	(3) (kN)	(4) (kN)	(5) (kN)
Specimen 01	44.12	58.28	124.00	234.75	457.42	116.50
Specimen 02	41.72	55.42	127.32	233.30	475.03	114.62
Specimen 03	43.78	49.50	121.41	237.35	465.74	126.55
Specimen 04	39.01	51.78	117.13	248.66	444.48	123.90
Specimen 05	44.99	45.28	116.07	232.20	467.95	113.26
Specimen 06	38.57	55.75	120.17	234.17	473.37	116.71
Specimen 07	41.31	58.63	115.40	245.42	457.61	114.79
Specimen 08	39.72	57.17	119.93	232.79	450.49	129.19
Specimen 09	38.37	52.22	117.32	238.97	451.53	117.72
Specimen 10	46.65	53.81	122.23	234.83	467.97	114.29
Average	41.82	53.78	120.10	237.24	461.16	118.75
$c_{v,Fmax}$	7.02%	7.81%	3.15%	2.36%	2.25%	4.78%
m_y	3.73	3.98	4.79	5.47	6.13	4.78
s_y	0.07	0.08	0.03	0.02	0.02	0.05
$F_{max,0.05}$	36.50	45.94	113.05	226.80	441.55	108.42

Appendix C. Additional results for the compression tests on TT

The box-plot in Fig. C.14f represents the median with the red central mark, and the 25th and 75th percentiles with the bottom and top edges of the box. It displays the distribution of datas for each specimen type.

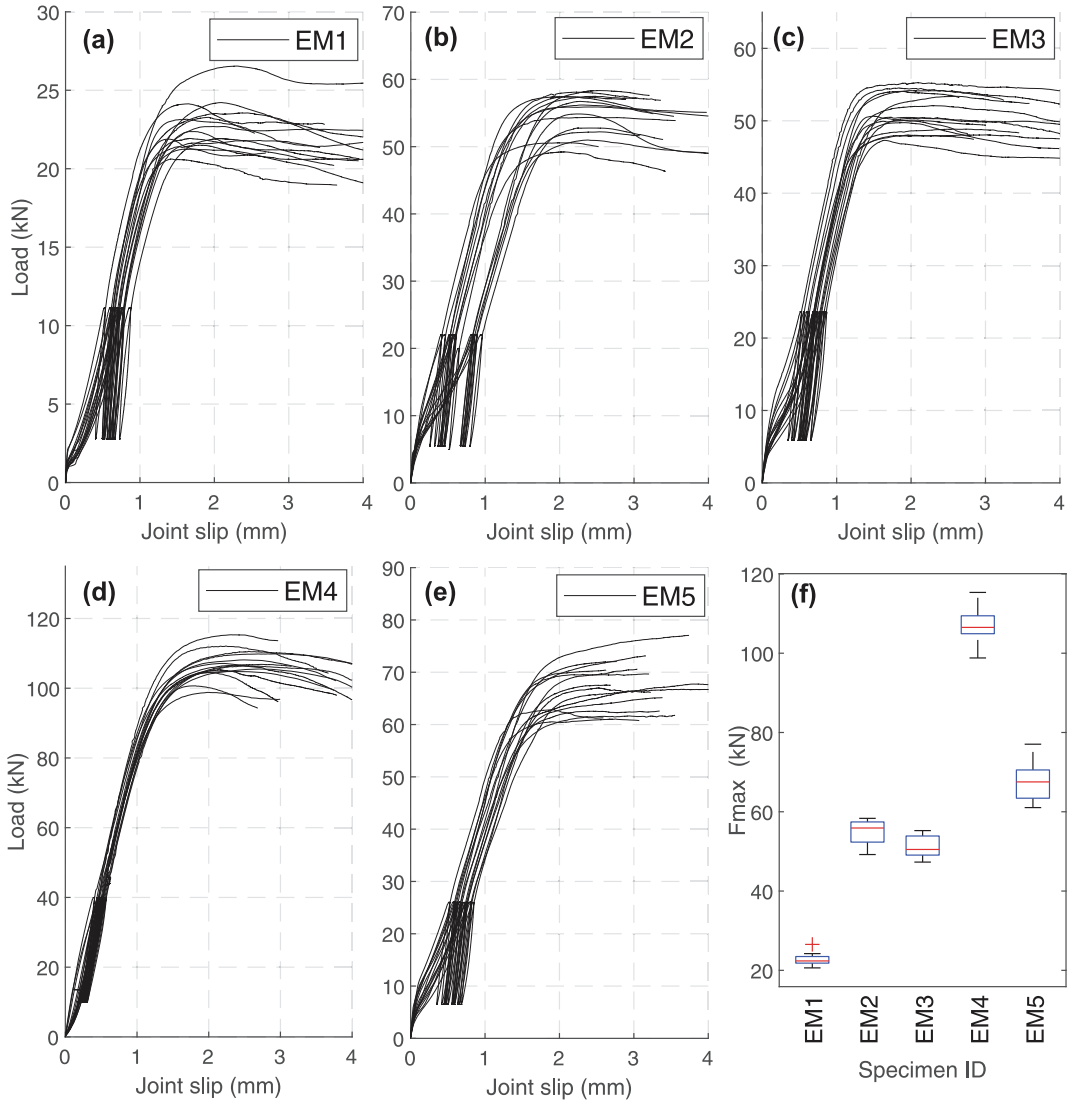

Fig. C.14. Load–displacement curves of all specimens for the compression tests: (a) EM1/ (b) EM2/ (c) EM3/ (d) EM4/ (e) EM5/ (f) Box-plot of the maximum load (F_{max}) per specimen type.

Appendix D. Additional results for the shear tests on TT

See Figs. D.15–D.20.

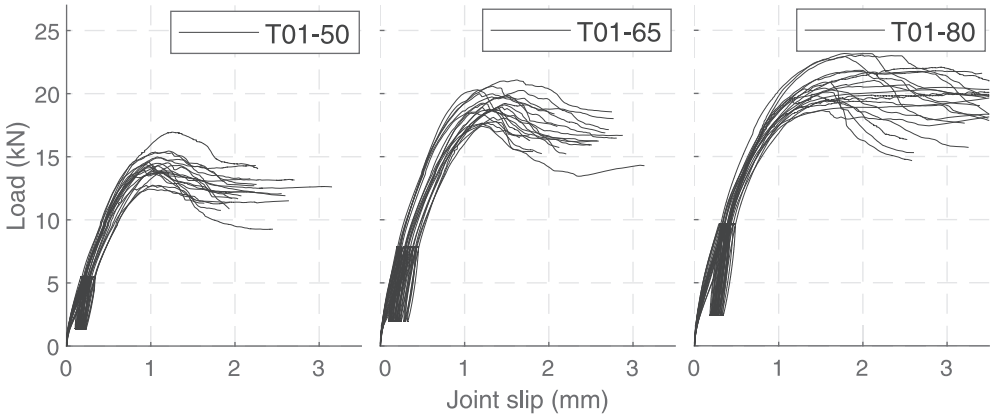

Fig. D.15. Load–displacement curves of T1.

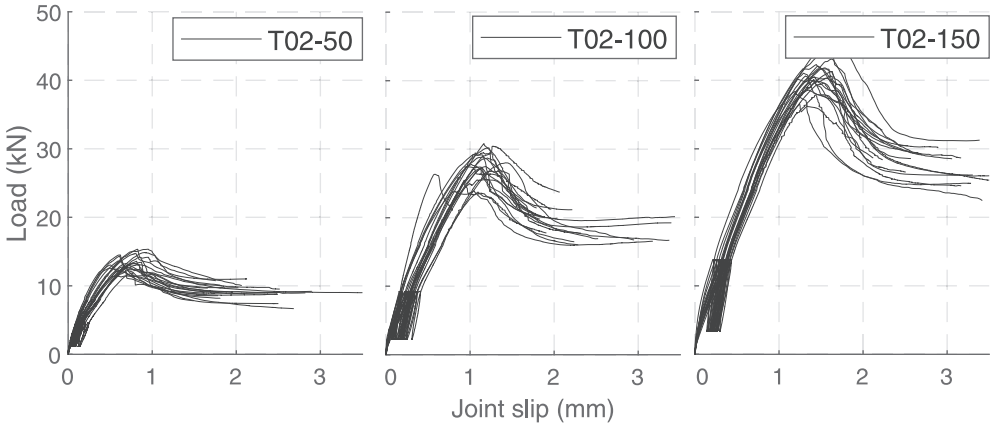

Fig. D.16. Load–displacement curves of T2.

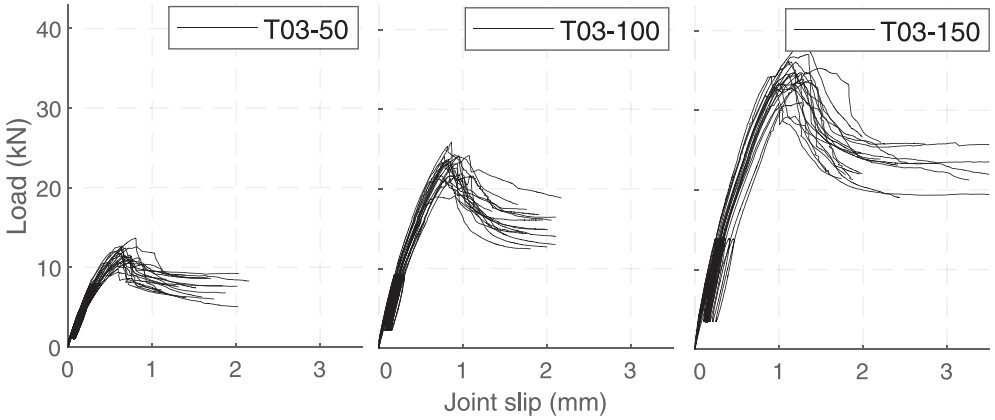

Fig. D.17. Load–displacement curves of T3.

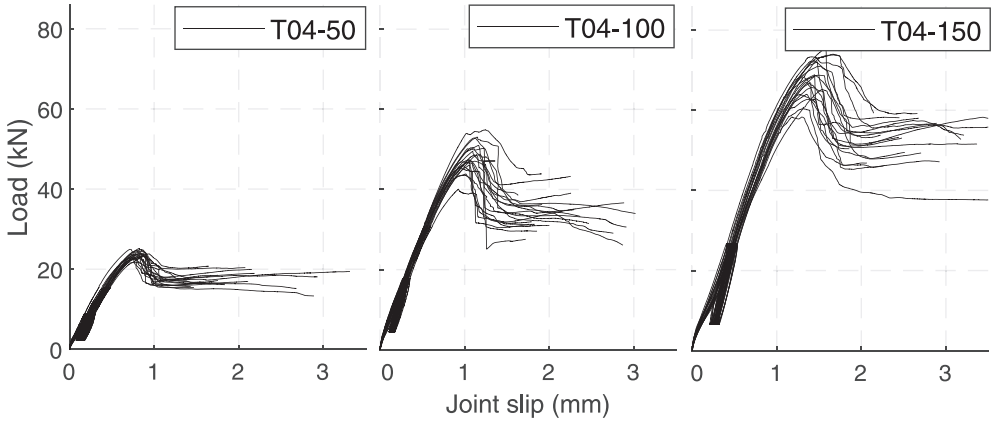

Fig. D.18. Load–displacement curves of T4.

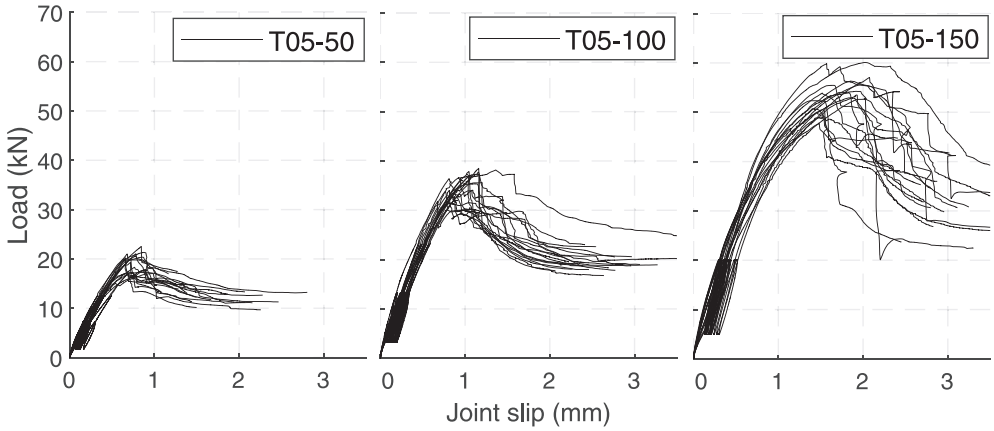

Fig. D.19. Load–displacement curves of T5.

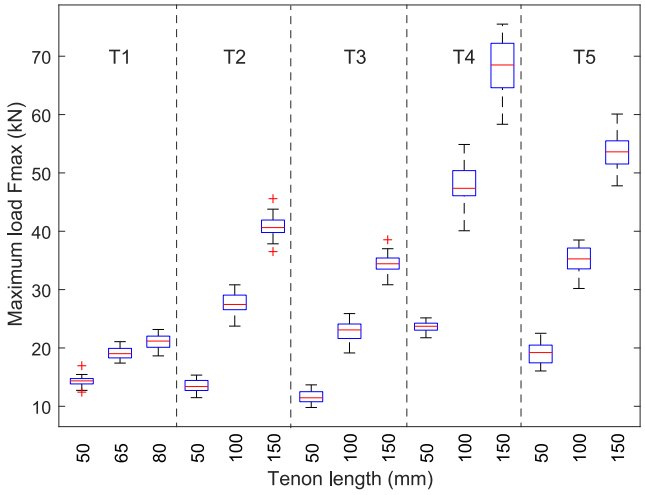

Fig. D.20. Boxplot of F_{max} values per specimen type for the shear tests.

References

[1] Robeller C. Timber plate shell structures: a digital resurgence of traditional joining methods. Springer International Publishing; 2019. p. 1117–33. doi:10.1007/978-3-030-03676-8_45.

[2] Schindler C. Information-Tool-Technology Contemporary digital fabrication as part of a continuous development of process technology as illustrated with the example of timber construction. Proceedings of the 27th ACADIA conference,. Halifax, Canada: Association for Computer Aided Design in Architecture; 2007. Researchgate link: https://www.researchgate.net/publication/268030070_Information-Tool-Technology_Contemporary_digital_fabrication_as_part_of_a_continuous_development_of_process_technology_as_illustrated_with_the_example_of_timber_construction/citations.

[3] Schwinn T, Krieg OD, Menges A. Robotically Fabricated Wood Plate Morphologies, Robotic prefabrication of a biomimetic, geometrically differentiated, lightweight, finger joint timber plate structure. In: Brell-Çokcan S, Braumann J, editors. Rob — Arch 2012: robotic fabrication in architecture, art, and design Vienna, Vienna: Springer; 2013. p. 48–61. https://doi.org/10.1007/978-3-7091-1465-0_4.

[4] Robeller C. Integral mechanical attachment for timber folded plate structures, Ph.D. thesis, École Polytechnique Fédérale de Lausanne. Lausanne 2015. https://doi.org/10.5075/epfl-thesis-6564.

[5] Li J-M, Knippers J. Segmental timber plate shell for the Landesgartenschau exhibition hall in Schwäbisch Gmönd–the application of finger joints in plate structures. Int J Space Struct 2015;30(2):123–39. https://doi.org/10.1260/0266-3511.30.2.123.

[6] Robeller C, Gamerro J, Weinand Y. Théâtre Vidy Lausanne – a double-layered timber folded plate structure. J Int Assoc Shell Spatial Struct 2017;58(4):295–314. https://doi.org/10.20898/j.iass.2017.194.864.

[7] Robeller C, Konakovic MA, Dedijer M, Pauly M, Weinand Y. A double-layered timber plate shell - computational methods for assembly, prefabrication, and structural design. Adv Archit Geometry 2016; 5:(9):104–22. doi:10.3218/3778-4. http://infoscience.epfl.ch/record/221313.

[8] Roche SN. Semi-rigid moment-resisting behavior of multiple tab-and-slot joint for freeform timber plate structures, Ph.D. thesis. École Polytechnique Fédérale de Lausanne, Lausanne 2017. https://doi.org/10.5075/epfl-thesis-8236.

[9] Gamerro J, Robeller C, Weinand Y. Rotational mechanical behaviour of wood-wood connections with application to double-layered folded timber-plate structure. Constr. Build. Mater. 2018;165:434–42. https://doi.org/10.1016/j.conbuildmat.2017.12.178.

[10] Sass L, Botha M. The instant house: a model of design production with digital fabrication. Int J Archit Comput 2006;4(4):109–23. https://doi.org/10.1260/147807706779399015.

[11] Albright D, Blouin V, Harding D, Heine U, Huette N, Pastre D. Sim[ply]: Sustainable construction with prefabricated plywood componentry. Procedia Environ Sci 2017; 38:760–4, sustainable synergies from Buildings to the Urban Scale. doi: 10.1016/j.proenv.2017.03.159. http://www.sciencedirect.com/science/article/pii/S1878029617301706.

[12] Gamerro J, Lemaître I, Weinand Y. Mechanical characterization of timber structural elements using integral mechanical attachments. In: World conference on timber engineering, Seoul, Republic of Korea; 2018. doi:10.5075/epfl-ibois-256646. http://infoscience.epfl.ch/record/256646.

[13] EN 1995-1-1:2004 - Eurocode 5: Design of timber structures - Part 1–1: General - Common rules and rules for buildings. European Committee for Standardization, 2004.

[14] SIA 265:2012. Timber Structures. Swiss society of engineers and architects, Zürich, 2012.

[15] DIN 1052:2004 - Design of timber structures – General rules and rules for buildings. German Institute for Standardization, 2004.

[16] Branco JM, Piazza M, Cruz PJ. Experimental evaluation of different strengthening techniques of traditional timber connections. Eng Struct 2011;33(8):2259–70. https://doi.org/10.1016/j.engstruct.2011.04.002.

[17] Branco JM, Descamps T. Analysis and strengthening of carpentry joints. Construct Build Mater 2015; 97: 34–47, special Issue: Reinforcement of Timber Structures. doi: 10.1016/j.conbuildmat.2015.05.089. http://www.sciencedirect.com/science/article/pii/S0950061815006029.

[18] Pang S-J, Oh J-K, Park J-S, Park C-Y, Lee J-J. Moment-carrying capacity of dovetailed mortise and tenon joints with or without beam shoulder. J Struct Eng 2011;137(7):785–9. https://doi.org/10.1061/(ASCE)ST.1943-541X.0000323.

[19] Koch H, Eisenhut L, Seim W. Multi-mode failure of form-fitting timber connections – experimental and numerical studies on the tapered tenon joint. Eng Struct 2013;48:727–38. https://doi.org/10.1016/j.engstruct.2012.12.002.

[20] Feio AO, Lourenço PB, Machado JS. Testing and modeling of a traditional timber mortise and tenon joint. Mater Struct 2014;47(1):213–25. https://doi.org/10.1617/s11527-013-0056-y.

[21] Claus T, Seim W, Schröder B. Multiple tenons – experimental study on load-bearing capacity and deformation characteristics. In: World conference on timber engineering, Vienna, Austria; 2016. p. 701–7.

[22] Schmidt T, Blass HJ. Contact joints in engineered wood products. World conference on timber engineering. Vienna: Austria; 2016. p. 8.

[23] Schmidt T, Blass HJ. Recent development in CLT connections part I: in-plane shear connection for CLT bracing elements under static loads, Wood and Fiber. Science 50 (CLT Mass Timber) 2018;48–57https://wfs.swst.org/index.php/wfs/article/view/2635/2422.

[24] Schmidt T, Blass HJ. Recent development in CLT connections part II: in-plane shear connections for CLT bracing elements under cyclic loads, Wood and Fiber. Science 50 (CLT Mass Timber) 2018;58–67https://wfs.swst.org/index.php/wfs/article/view/2636/2423.

[25] Claus T, Riehle T, Seim W, Gotz T. Interlocking shear wall connections. In: World conference on timber engineering, Seoul, Republic of Korea;, 2018. https://www.uni-kassel.de/fb14bau/uploads/media/CLAUS_RIEHLE_SEIM_GÖTZ_INTERLOCKING_SHEAR_WALL_CONNECTIONS.pdf.

[26] Siem J, Jorissen A. Can traditional carpentry joints be assessed and designed using modern standards. International conference on structural health assessment of timber structures. 2015. p. 9–11.

[27] Verbist M, Branco JM, Poletti E, Descamps T, Lourenço PB. Single Step Joint: overview of European standardized approaches and experimentations. Mater Struct 50 (2). doi:10.1617/s11527-017-1028-4. http://link.springer.com/10.1617/s11527-017-1028-4.

[28] EN 408. Timber structures – structural timber and glued laminated timber – determination of some physical and mechanical properties. European Committee for Standardization (CEN); 2010.

[29] EN 16351:2015. Timber structures – cross laminated timber – requirements. European Committee for Standardization (CEN); 2015.

[30] EN 789. Timber structures – test methods – determination of mechanical properties of wood based panels. European Committee for Standardization (CEN); 2004.

[31] NF. Laminated bonded wood – test of compression shear B51–. French Association for Standardization (AFNOR); 1981. p. 032.

[32] Rad AR, Weinand Y, Burton H. Experimental push-out investigation on the in-plane force-deformation behavior of integrally-attached timber through-tenon joints. Construction and Building Materials 2019;215:925–40. https://doi.org/10.1016/j.conbuildmat.2019.04.156.

[33] Dedijer M, Roche SN, Weinand Y. Shear resistance and failure modes of edgewise Multiple Tab-and-Slot Joint (MTSJ) connection with dovetail design for thin LVL spruce plywood Kerto-Q panels. World conference on timber engineering. 2016.

[34] EN 12369–1. Wood-based panels – characteristic values for structural design – Part 1: OSB, particleboards and fiberboards. European Committee for Standardization (CEN); 2001.

[35] VTT Certificate No. 184/03. Kerto LVL. VTT Research Centre of Finland, Espoo, updated 17 May 2016. https://www.metsawood.com/global/Tools/MaterialArchive/MaterialArchive/Kerto-VTT-C-184-03-Certificate.pdf.

[36] Blaß HJ, Streib J. Baubuche beech laminated veneer lumber – design assistance for drafting and calculation in accordance with eurocode 5; 2017.http://pollmeier.com/en/downloads/design-manual.html [accessed: 17–05-2019].

[37] Dold Holzwerke GmbH, Panneaux 3-plis et 5-plis; 2008. http://doldholz.homepage.t-online.de/doldweb/images/stories/dold/franz.%20-%203-s%20prospekt%20mehrseiter.pdf.

[38] EN 323:1993. Wood-based panels. Determination of density. European Committee for Standardization (CEN); 1993.

[39] Walter + Bai AG, Universal testing machine model LFV; 2020. https://www.walterbai.com/page/products/Materials_Testing_Systems/Combined_Axial-Torsional_Testing_System/LFV_Series_Servohydraulic_Systems.php.

[40] EN 26891. Timber structures – joints made with mechanical fasteners – general principles for the determination of strength and deformation characteristics. European Committee for Standardization (CEN); 1991.

[41] Leitz user lexicon. Lexicon Ed 2011;6:428https://www.hoechsmann.com/en/lexikon/23836/Leitz-Anwenderlexikon.

[42] ISO 554:1976. Standard atmospheres for conditioning and, or testing - Specifications. International Organization for Standardization; 1976.

[43] Dietsch P, Winter S. Eurocode 5–future developments towards a more comprehensive code on timber structures. Struct Eng Int 2012;22(2):223–31. https://doi.org/10.2749/101686612X13291382991001.

[44] EN. 2003–03 – Eurocode 0: Basis of structural design – Annex D - Design assisted by testing. European Committee for Standardization; 1990.

[45] Hunt RD, Bryant AH. Statistical implications of methods of finding characteristic strengths. J Struct Eng 1996;122(2):202–9. https://doi.org/10.1061/(ASCE)0733-9445(1996)122:2(202).

[46] Köhler J, Sørensen JD, Faber MH. Probabilistic modeling of timber structures. Struct Saf 2007; 29 (4): 255–67, probabilistic Concepts in the Design of Timber Structures. doi:10.1016/j.strusafe.2006.07.007. http://www.sciencedirect.com/science/article/pii/S0167473006000476.

[47] Gamerro J, Bocquet JF, Weinand Y. Dataset of the paper: “Experimental investigations on the load-carrying capacity of digitally produced wood-wood connections”. Mendeley Data 2020;V1. https://doi.org/10.17632/trpf7c56cb.1.